

Right ventricular remodeling in idiopathic and scleroderma-associated pulmonary arterial hypertension: two distinct phenotypes

Benjamin W. Kelemen,^{1,a} Stephen C. Mathai,^{1,a} Ryan J. Tedford,² Rachel L. Damico,¹ Cecilia Corona-Villalobos,³ Todd M. Kolb,¹ Neal F. Chaisson,¹ Traci Houston Harris,¹ Stefan L. Zimmerman,³ Ihab R. Kamel,³ David A. Kass,² Paul M. Hassoun¹

¹Division of Pulmonary and Critical Care Medicine, Johns Hopkins University School of Medicine, Baltimore, Maryland, USA; ²Division of Cardiology, Department of Medicine, Johns Hopkins University School of Medicine, Baltimore, Maryland, USA; ³Department of Radiology and Radiological Sciences, Johns Hopkins University School of Medicine, Baltimore, Maryland, USA; *These authors contributed equally to this article.

Abstract: Patients with scleroderma (SSc)-associated pulmonary arterial hypertension (PAH) have worse survival than patients with idiopathic PAH (IPAH). We hypothesized that the right ventricle (RV) adapts differently in SSc-PAH versus IPAH. We used cardiac magnetic resonance imaging (cMRI) and hemodynamic characteristics to assess the relationship between RV morphology and RV load in patients with SSc-PAH and IPAH. In 53 patients with PAH (35 with SSc-PAH and 18 with IPAH) diagnosed by right heart catheterization (RHC), we examined cMRIs obtained within 48 hours of RHC and compared RV morphology between groups. Regression analysis was used to assess the association between diagnosis (IPAH vs. SSc-PAH) and RV measurements after adjusting for age, sex, race, body mass index (BMI), left ventricular (LV) mass, and RV load. There were no significant differences in unadjusted comparisons of cMRI measurements between the two groups. Univariable regression showed RV mass index (RVMI) was linearly associated with measures of RV load in both the overall cohort and within each group. Multivariable linear regression models revealed a significant interaction between disease type and RVMI adjusting for pulmonary vascular resistance (PVR), age, sex, race, BMI, and LV mass. This model showed a decreased slope in the relationship between RVMI and PVR in the SSc-PAH group compared with the IPAH group. RVMI varies linearly with measures of RV load. After adjusting for multiple potential confounders, patients with SSc-PAH demonstrated significantly less RV hypertrophy with increasing PVR than patients with IPAH. This difference in adaptive hypertrophy may in part explain previously observed decreased contractility and poorer survival in SSc-PAH.

Keywords: pulmonary arterial hypertension, scleroderma, right ventricle, cardiac magnetic resonance imaging.

Pulm Circ 2015;5(2):327-334. DOI: 10.1086/680356.

Pulmonary arterial hypertension (PAH), or group 1 disease of the World Health Organization (WHO) classification of pulmonary hypertension (PH), is defined by a mean pulmonary artery pressure (mPAP) ≥ 25 mmHg and pulmonary vascular resistance (PVR) ≥ 3 Wood units in the absence of significant left-sided disease (pulmonary capillary wedge pressure [PCWP] ≤ 15 mmHg), parenchymal lung disease, or chronic thromboembolic disease.¹ PAH includes, among other entities, idiopathic PAH (IPAH) and PAH associated with connective tissue diseases (CTDs); scleroderma (SSc), a heterogeneous disease characterized by dysfunction of the endothelium, dysregulation of fibroblasts, and abnormalities of the immune system, leads to progressive fibrosis of the skin and internal organs and is the most common CTD associated with PAH.¹ SSc-associated PAH (SSc-PAH) occurs in 8%–12% of all cases of SSc

and, along with interstitial lung disease, represents the leading cause of mortality in this disease.²⁻⁴ Despite having similar measures of right ventricular (RV) load,^{5,6} patients with SSc-PAH have worse survival and poorer response to treatment compared with patients with IPAH.^{7,8} In investigating this apparent paradox, we and others have shown that RV function differs between SSc-PAH and IPAH and strongly predicts survival, indicating the importance of the RV in maintaining adequate cardiac output (CO) in the face of increased RV load.⁹⁻¹¹

Recent work from our group has investigated direct measurements of RV contractility using pressure volume loops in the RV to compare IPAH with SSc in patients with and without PH.¹² In this study, we found the ratio of end-systolic elastance to effective arterial elastance, a measure of RV-pulmonary arterial coupling, to

Address correspondence to Dr. Stephen C. Mathai, Johns Hopkins University, Division of Pulmonary and Critical Care Medicine, 1830 East Monument Street, Baltimore, MD 21205, USA. E-mail: smathai4@jhmi.edu. Presented in part: 23rd Annual European Respiratory Society Meeting; Barcelona, Spain; September 7–11, 2013 (Abstract A4835).

Submitted August 18, 2014; Accepted October 13, 2014; Electronically published April 30, 2015.

© 2015 by the Pulmonary Vascular Research Institute. All rights reserved. 2045-8932/2015/0502-0012. \$15.00.

be significantly decreased in patients with SSc and PAH as compared with patients with IPAH and patients with SSc without PAH. These data strongly suggest differences in RV intrinsic contractility between patients with IPAH and patients with SSc-PAH that become apparent in the setting of an increased afterload. Because SSc is characterized by endothelial dysfunction and microvascular disease, we hypothesized on the basis of microvascular-myocyte imbalance that patients with SSc-PAH, compared with patients with IPAH, may display maladaptive RV hypertrophy as assessed by RV mass in response to increased pulmonary vascular load.

Although echocardiography is a useful screening modality in pulmonary hypertension, cardiac magnetic resonance imaging (cMRI) has been an increasingly valuable tool in assessing cardiac morphology and function and in determining prognosis in PAH.^{13,14} Echocardiography is an operator-dependent and two-dimensional method that relies on geometric assumptions for volume and mass calculations. In addition, results are highly dependent on patient and probe position, which is variable between patients.^{15,16} cMRI provides a true three-dimensional image and is considered the gold standard, with no operator dependence or dependence on optimal imaging windows. Therefore, we used cMRI to test our hypothesis and assess the relationship between RV mass and RV load in two distinct PAH disease states: SSc-PAH and IPAH.

METHODS

This prospective study was Health Insurance Portability and Accountability Act compliant and was approved by the institutional review board at Johns Hopkins Hospital. We performed a cross-sectional analysis of prospectively gathered data from a cohort of 53 patients with SSc-PAH and IPAH. Eighteen patients received a diagnosis of IPAH. Of these 18 patients, 1 patient with known IPAH had a PCWP of 16 at the time of right heart catheterization (RHC). This was attributed to septal interdependence in the setting of significant volume overload. Another patient had a confirmed diagnosis of IPAH but had achieved normalized mPAP (<25 mmHg) with medication at the time of a repeat RHC. Patients were excluded if they had no PH, did not have WHO group 1 PAH, had renal or hepatic failure, and/or had decompensated heart failure that would preclude stability for cMRI. Patients underwent RHC and cMRI within 48 hours of each other.

RHC acquisition

The following hemodynamic data were collected: right atrial pressure (RAP), mPAP, CO, PCWP, and mixed venous oxygen saturation. Additional measurements that were calculated included PVR = $(\text{mPAP} - \text{PCWP})/\text{CO}$, estimated pulmonary arterial compliance (C_{PA} ; stroke volume/pulmonary pulse pressure), cardiac index (CI; CO/body surface area), and RV stroke volume index (stroke volume/body surface area). RV load parameters assessed were mPAP, PVR, and C_{PA} .

cMRI acquisition

cMRI imaging was performed on a 3-T MRI system (Magnetom Trio, Siemens Healthcare, Erlangen, Germany). cMRI protocol in-

cluded breath-hold cine short-axis and four-chamber images with retrospective gating at 3-T using a body coil array.

Cine short-axis images. Segmented gradient echo (FLASH) cine short-axis images including both ventricles from base to apex were acquired. Sequence parameters included repetition time/echo time (TR/TE) of 64.2/2.97 ms; slice thickness of 6 mm; flip angle of 18°; and acquisition matrix of 256×192 .

Cine four-chamber images. Cine four-chamber images were obtained with a retrospectively gated segmented gradient-echo sequence (FLASH). Sequence parameters included TR/TE of 52.2/2.82 ms; slice thickness of 8 mm; flip angle of 12°; and acquisition matrix of 256×192 .

Image analysis

Assessment of the RV function with three-dimensional measures was performed using contiguous short-axis cine images covering the entire RV and LV. The RV and LV epicardial and endocardial ventricular borders were manually contoured in end systole and end diastole for functional analysis by Simpson's method. Ejection fraction was calculated for RV and LV. RV and LV mass were measured according to the following equation: ventricular mass = 1.05 (epicardial volume – endocardial volume). The interventricular septum was excluded from the RV mass and included in the LV mass. Functional parameters were normalized to body surface area; these included end-diastolic and end-systolic volumes, stroke volume, CO, and ventricular mass. RV mass index (RVMI), RV end-diastolic volume index (RVEDVI), and volume mass index (VMI) were chosen as measures of RV remodeling on the basis of earlier literature demonstrating associations between changes in these parameters and increases in RV afterload.^{13,17,18} The RV is expected to hypertrophy in response to increased afterload on the basis of the law of Laplace; however, because no validated description of patterns of cMRI-assessed RV hypertrophy in PAH exists, RVMI serves as a surrogate for RV hypertrophy. Similarly, increases in RVEDVI are associated with decreased RV function, whereas VMI, the ratio of RV mass to LV mass, increases in response to RV afterload, reflecting relative increases in RV mass. VMI was calculated from the RV and LV mass in diastole: $\text{VMI} = \text{RV mass}/\text{LV mass}$.

Statistical analysis

Statistical analysis was performed with STATA/IC software (vers. 12.1, College Station, TX). Variables were summarized using mean \pm 95% confidence interval. Wilcoxon ranked sum test was used to compare means between groups. Categorical variables were summarized and compared using the χ^2 statistic. Univariable linear regression was used to assess the association between cMRI measurements as the outcome and RV load. Collinearity was assessed by variance inflation factors, and variables were excluded from multivariable models based upon demonstration of collinearity. Multivariable linear regression (MLR) was used to assess the relationship between cMRI measurements as the outcome and RV load (mPAP, PVR, C_{PA}), age, sex, race, body mass index (BMI), end-diastolic LV mass index, and disease

Table 1. Clinical, demographic, and hemodynamic data

Variable	SSc-PAH (n = 35)	IPAH (n = 18)	P
Age, years, mean (\pm SD)	62 (9)	51 (12)	0.0006
Female sex	33 (94)	16 (89)	0.48
White race	32 (91)	15 (83)	0.38
BMI, mean (\pm SD)	26.2 (5.9)	32.1 (6.9)	0.004
No. of PAH-specific medications			
0	22 (63)	0 (0)	<0.001
1	13 (37)	17 (94)	
2	0 (0)	1 (6)	
WHO functional class			
I	0 (0)	6 (33)	0.005
II	15 (47)	7 (39)	
III	16 (50)	5 (28)	
IV	1 (3)	0 (0)	
RAP, mmHg, mean (\pm SD)	7 (4)	8 (5)	0.57
mPAP, mmHg, mean (\pm SD)	39 (12)	46 (17)	0.10
PCWP, mmHg, mean (\pm SD)	9 (3)	10 (3)	0.19
CO, L/min, mean (\pm SD)	4.4 (1.4)	5.2 (1.3)	0.05
CI, L/min/m ² , mean (\pm SD)	2.6 (0.8)	2.7 (0.5)	0.65
PVR, Wood units, mean (\pm SD)	8.4 (5.9)	7.6 (4.0)	0.59
C _{PA} , mL/mmHg, mean (\pm SD)	1.76 (1.24)	1.81 (1.12)	0.91

Note: Data are no. (%) of patients, unless otherwise indicated. SSc-PAH: scleroderma-associated pulmonary arterial hypertension; IPAH: idiopathic pulmonary arterial hypertension; SD, standard deviation; BMI: body mass index, calculated as weight in kilograms divided by the square of height in meters; PAH: pulmonary arterial hypertension; WHO: World Health Organization; RAP: right atrial pressure; mPAP: mean pulmonary artery pressure; PCWP: pulmonary capillary wedge pressure; CO: cardiac output; CI: cardiac index; PVR: pulmonary vascular resistance; C_{PA}: pulmonary artery compliance.

Table 2. Unadjusted cardiac magnetic resonance imaging data

Variable	SSc-PAH (n = 35)	95% CI	IPAH (n = 18)	95% CI	P
RV mass, g	58.8	47.8–69.9	65.9	48.0–83.8	0.47
RV mass index, g/m ²	34.4	27.9–40.9	34.5	24.7–44.3	0.98
RVEDV, mL	148.9	130.4–167.5	174.5	147.5–201.5	0.11
RVEDV index, mL/m ²	88.1	76.3–99.8	90.1	75.8–104.7	0.83
RVEF, %	46.0 (n = 31)	41.1–50.9	41.6 (n = 17)	34.4–48.9	0.29
RVSV, mL	65.1 (n = 31)	57.8–72.5	69.1 (n = 17)	58.7–79.5	0.52
RVSV index, mL/m ²	38.4 (n = 31)	34.4–42.3	35.2 (n = 17)	31.1–39.2	0.29
RV CO, L/min	4.79 (n = 31)	4.32–5.25	5.21 (n = 17)	4.38–6.03	0.32
TAPSE, cm	14.3 (n = 28)	11.9–16.7	14.4 (n = 16)	11.4–17.4	0.96
VMI	0.51 (n = 35)	0.42–0.59	0.62 (n = 17)	0.45–0.79	0.17

Note: All data are mean values unless otherwise indicated. SSc-PAH: scleroderma-associated pulmonary arterial hypertension; IPAH: idiopathic pulmonary arterial hypertension; RV: right ventricular; RVEDV: right ventricular end-diastolic volume; RVEF: right ventricular ejection fraction; RVSV: right ventricular stroke volume; RV CO: right ventricular cardiac output; TAPSE: tricuspid annular plane systolic excursion; VMI: ventricular mass index.

Table 3. Univariable linear regression: right ventricular mass index

Predictor	Coefficient (95% CI)	<i>P</i>
mPAP, mmHg	0.02 (0.01–0.03)	0.001
PVR, Wood units	0.05 (0.02–0.08)	<0.001
C _{PA} , mL/mmHg	–0.22 (–0.34 to –0.10)	0.001
Age, years	–0.003 (–0.02 to 0.01)	0.65
Sex, female vs. male	0.11 (–0.49 to 0.71)	0.71
Race, white vs. black	–0.28 (–0.53 to 0.47)	0.91
BMI	–0.01 (–0.03 to 0.01)	0.49
No. of PAH medications	0.14 (–0.16 to 0.44)	0.35

Note: Coefficient reported as mean change in predictor per log g/m² of right ventricular mass index with 95% confidence interval (CI). mPAP: mean pulmonary artery pressure; PVR: pulmonary vascular resistance; C_{PA}: pulmonary artery compliance; BMI: body mass index, calculated as weight in kilograms divided by the square of height in meters; PAH: pulmonary arterial hypertension.

state (IPAH vs. SSc-PAH) as predictors. Predictors were selected on the basis of earlier studies demonstrating significant associations between these parameters and MRI measures of RV structure.^{19,20} Outcomes were assessed for normality of distribution and transformed as necessary to meet the assumptions of MLR. Interaction models assessing whether the relationship between RVMI and RV load differed by disease state were created on the basis of the results of MLR models; a *P* value <0.10 was considered significant for these analyses.²¹

RESULTS

Patient demographic characteristics

Comparing the clinical characteristics of the two cohorts, several differences were found (Table 1). Although patients with SSc-PAH were significantly older and less likely to be obese than the patients with IPAH, there were no significant differences in the sex or race distribution between cohorts. Patients with SSc-PAH were more likely to be treatment naive, whereas all patients with IPAH were receiving treatment at the time of RHC. Patients with SSc-PAH had worse functional status at the time of catheterization, with more patients experiencing WHO functional class 3 or 4 symptoms (53% and 28% for SSc-PAH and IPAH, respectively; *P* = 0.005).

Hemodynamic measurements

Invasive hemodynamic measurements differed minimally between the two groups (Table 2). On average, patients with SSc-PAH tended to have a lower mPAP and had significantly lower CO than their IPAH counterparts. However, CI did not differ between the two groups, suggesting that body size accounted for the observed difference in CO. Moreover, RV load as assessed by PVR and C_{PA} did not differ between the two groups.

cMRI measurements

There were no significant differences between the unadjusted means of the cMRI measurements between the two groups (Table 3).

Patients with SSc-PAH and IPAH had similar RV mass and RV end-diastolic volume when compared as individual measures, indexed to body surface area or indexed to each other as VMI. There was no significant difference in terms of measures of RV function, such as RV ejection fraction (RVEF), RV stroke volume, or tricuspid annular plane systolic excursion (TAPSE).

Univariable linear regression analysis revealed significant relationships between measures of RV load (mPAP, PVR, and compliance) and cMRI measurements of RV mass (RVMI and VMI; Tables 3, 4). Neither RVMI nor VMI were associated with age, sex, race, BMI, or number of PAH-specific medications that patients were receiving before the cMRI. RVEDVI was not associated with any measures of RV load, age, sex, race, or BMI (Table 5). However, there was a positive linear association between RVEDVI and the total number of PAH-specific medications subjects had been exposed to before enrollment. Because there was no association between RV load and RVEDVI, MLR models were not assessed.

Multivariable analysis stratifying by diagnosis revealed that, after adjusting for age, sex, race, and BMI, PVR and LV mass were strongly associated with RVMI, whereas only PVR was associated with VMI in these adjusted models (Tables 6, 7). In these stratified analyses, disease state (SSc-PAH or IPAH) seemed to modify the relationship between cMRI measurements and RV load. As shown in figures 1 and 2, the slopes of the relationship between RVMI and RV load and between VMI and RV load visually differed. When examining for interaction between RV load and disease type, a significant association was found for both RVMI and VMI (*P* value for interaction = 0.04 and 0.03, respectively), suggesting that there was less RV remodeling (as assessed by RVMI and VMI) in patients with SSc-PAH compared with patients with IPAH with increasing PVR. These findings were confirmed in sensitivity analyses

Table 4. Univariable linear regression: ventricular mass index (*n* = 52)

Predictor	Coefficient (95% CI)	<i>P</i>
mPAP, mmHg	0.02 (0.01–0.03)	<0.001
PVR, Wood units	0.06 (0.03–0.08)	<0.001
C _{PA} , mL/mmHg	–0.25 (–0.34 to –0.16)	<0.001
Age, years	–0.002 (–0.014 to 0.01)	0.69
Sex, female vs. male	0.37 (–0.11 to 0.86)	0.13
Race, white vs. black	0.11 (–0.38 to 0.61)	0.65
BMI	0.001 (–0.02 to 0.02)	0.92
No. of PAH medications	0.14 (–0.12 to 0.39)	0.29

Note: Coefficient reported as mean change in predictor per log unit change in ventricular mass index with 95% confidence interval (CI). mPAP: mean pulmonary artery pressure; PVR: pulmonary vascular resistance; C_{PA}: pulmonary artery compliance; BMI: body mass index, calculated as weight in kilograms divided by the square of height in meters; PAH: pulmonary arterial hypertension.

Table 5. Univariable linear regression: outcome right ventricular end-diastolic volume index

Predictor	Coefficient (95% CI)	P
mPAP, mmHg	0.005 (−0.001 to 0.01)	0.12
PVR, Wood units	0.01 (−0.004 to 0.03)	0.16
C _{PA} , mL/mmHg	−0.05 (−0.11 to 0.02)	0.19
Age, years	−0.002 (−0.01 to 0.005)	0.56
Sex, female vs. male	0.11 (−0.20 to 0.41)	0.49
Race, white vs. black	−0.02 (−0.27 to 0.24)	0.89
BMI	−0.01 (−0.02 to 0.01)	0.31
No. of PAH medications	0.17 (0.02–0.31)	0.03

Note: Coefficient reported as mean change in predictor per log mL/m² of right ventricular end-diastolic volume index with 95% confidence interval (CI). mPAP: mean pulmonary artery pressure; PVR: pulmonary vascular resistance; C_{PA}: pulmonary artery compliance; BMI: body mass index, calculated as weight in kilograms divided by the square of height in meters; PAH: pulmonary arterial hypertension.

that excluded two subjects with IPAH who did not meet strict criteria for PAH, as noted in the “Methods” section.

DISCUSSION

In this study, we examined the relationship between RV morphology and pulmonary vascular mechanics in patients with PAH, specifically focusing on the relationship between measures of RV remodeling (RVMI and VMI) and measures of RV load (mPAP, PVR, and C_{PA}) in subjects with IPAH and SSc-PAH. We hypothesized that the RV adapts differently in SSc-PAH compared with IPAH, leading to different RV morphology between the two disease

states as assessed by cMRI. We found that the relationship between RV remodeling and RV load was modified by disease state, because patients with SSc-PAH demonstrated significantly less RV hypertrophy with increasing PVR after adjusting for differences in RV load, age, sex, race, BMI, and LV mass.

The response of the RV to increased load is the primary determinant of outcome in PAH.²² Earlier cohort studies have demonstrated improved outcomes in adult patients with PAH related to Eisenmenger syndrome (ES) compared with patients with IPAH and have attributed this improved survival in part to better adaptation of the RV, evidenced by hypertrophy and increased RV mass.²³⁻²⁶ Similarly, Rich and colleagues²⁷ have noted differences in RV size and morphology when contrasting the postmortem RVs of a long-term survivor and a short-term survivor with IPAH, highlighting the importance of RV hypertrophic response to increased afterload. These observations suggest a potential relationship between RV hypertrophy and outcomes in PAH. However, as shown by van Wolferen and colleagues¹³ in a large cohort of IPAH patients, neither RVMI at baseline nor change in RVMI at 1 year of follow-up predicts survival. Thus, other factors are likely involved in the relationship between RV mass and RV function. As shown in a recent study of an animal model of ES, RV adaptation to pressure overload occurs not only through RV hypertrophy but also through increased RV contractility, mediated through the Anrep effect (i.e., slow force contraction leading to proportional increase in ventricular inotropy in response to an increase in afterload) in the RV.²⁸ Whether this effect is present in patients with PAH or varies by disease type (e.g., ES vs. IPAH vs. SSc-PAH) remains unclear. Furthermore, RV mass may not be the best measure of RV adaptation to increased afterload, because afterload-dependent measures of RV function, such as TAPSE and RVEF, are strongly predictive of survival.⁹⁻¹¹

To our knowledge, the current study is the first to examine differences in the relationship between RV hypertrophy and after-

Table 6. Multivariable linear regression: outcome right ventricular mass index, stratified by diagnosis

Predictor	SSc-PAH		IPAH	
	β (95% CI)	P	β (95% CI)	P
PVR	0.05 (0.02–0.08)	<0.001	0.14 (0.03–0.25)	0.02
ED LV mass	0.02 (0.01–0.02)	0.001	0.03 (−0.001 to 0.05)	0.06
Age	0.01 (−0.01 to 0.03)	0.31	0.004 (−0.02 to 0.02)	0.68
Sex	−0.31 (−1.01 to 0.40)	0.38	−0.35 (−1.76 to 1.06)	0.59
Race	−0.17 (−0.72 to 0.38)	0.53	0.32 (−0.56 to 1.19)	0.43
BMI	0.01 (−0.02 to 0.04)	0.47	0.03 (−0.02 to 0.08)	0.22
Constant	1.46 (−0.08 to 3.00)	0.06	0.02 (−2.63 to 2.67)	0.99

Note: Coefficient reported as change in predictor per log g/m² of right ventricular mass index (RVMI) with 95% confidence interval (CI). SSc-PAH: scleroderma-associated pulmonary arterial hypertension; IPAH: idiopathic pulmonary arterial hypertension; PVR: pulmonary vascular resistance; ED LV mass: end-diastolic left ventricular mass index; BMI: body mass index, calculated as weight in kilograms divided by the square of height in meters.

Table 7. Multivariable linear regression, outcome ventricular mass index, stratified by diagnosis ($n = 52$)

Predictor	SSc-PAH		IPAH	
	β (95% CI)	P	β (95% CI)	P
PVR	0.04 (0.02–0.08)	0.001	0.14 (0.04 to 0.25)	0.02
ED LV mass	–0.002 (–0.01 to 0.01)	0.68	0.01 (–0.02 to 0.03)	0.53
Age	0.005 (–0.01 to 0.02)	0.51	0.004 (–0.02 to 0.02)	0.68
Sex	–0.25 (–0.90 to 0.40)	0.43	–0.40 (–1.79 to 0.99)	0.53
Race	0.002 (–0.56 to 0.57)	0.99	0.34 (–0.52 to 1.20)	0.39
BMI	0.01 (–0.01 to 0.03)	0.35	0.03 (–0.02 to 0.09)	0.18
Constant	–1.32 (–2.67 to 0.02)	0.06	–3.08 (–5.70 to 0.47)	0.03

Note: Coefficient reported as change in predictor per log unit change in ventricular mass index (VMI) with 95% confidence interval (CI). SSc-PAH: scleroderma-associated pulmonary arterial hypertension; IPAH: idiopathic pulmonary arterial hypertension; PVR: pulmonary vascular resistance; ED LV mass: end-diastolic left ventricular mass index; BMI: body mass index, calculated as weight in kilograms divided by the square of height in meters.

load in SSc-PAH and IPAH using cMRI. Patients with SSc-PAH had significantly less increase in RV mass as measured by both RVMI and VMI for a given increase in PVR, even when adjusting for multiple potential confounders (figs. 1, 2). Because our study is cross-sectional, we are unable to infer that the hypertrophy observed is a direct response to RV afterload. However, the clearly different slopes depicting the relationship between RVMI or VMI versus PVR in patients with SSc-PAH and IPAH suggests a difference in adaptive hypertrophy. Although there were no differences in resting hemodynamic measures or RVEF, whether this difference in RV remodeling is accompanied by other intrinsic changes in RV function is unknown. RV pump function is not yet well enough understood to classify hypertrophic changes as adaptive or maladaptive. Preliminary work from our group does not demonstrate a relationship between wall thickness and RV contractility measured using pressure-volume loops, despite showing relatively strong relationships between wall thickness and afterload.²⁹ However, earlier work has suggested that intrinsic RV function may differ between patients with SSc-PAH and patients with other forms of PAH.^{12,30} Specifically, studies using pressure volume loop measurements have shown differences in RV contractility and in mechanical coupling between the RV and the pulmonary artery in SSc-PAH, compared with IPAH.¹² Still, the etiology of this uncoupling remains unclear, although differences in adaptive hypertrophy could explain this discrepancy.

Of note, RV end-diastolic volume was not associated with RV afterload. This finding was surprising, because increasing RV end-diastolic volume has been shown to correlate with poor survival.¹⁷ Presumably, this relationship to outcome is through failure of RV contractility and RV compensation for increased RV afterload. The lack of correlation between RV afterload and RV end-diastolic volume may be explained by heterogeneity of intrinsic RV function in our cohort allowing for differential adaptation to elevated RV afterload. However, regression analysis stratified by diagnosis also re-

vealed no correlation between RV end-diastolic volume and measures of afterload.

Limitations

Our study is limited by its cross-sectional nature; thus, it is difficult to assess causality or, more importantly, the temporal nature of the phenomena observed. Whether the findings imply differences in the rate of hypertrophy or progression of increasing vascular load is unanswered. We did not examine qualitative differences in RV hypertrophy between groups. Unlike in the LV, where hypertrophic responses have been well-defined using echocardiography, adaptive and maladaptive RV hypertrophic responses are not well defined.^{22,31} Because RV hypertrophy can be inhomogeneous, measures of gross RV mass do not distinguish between functionally

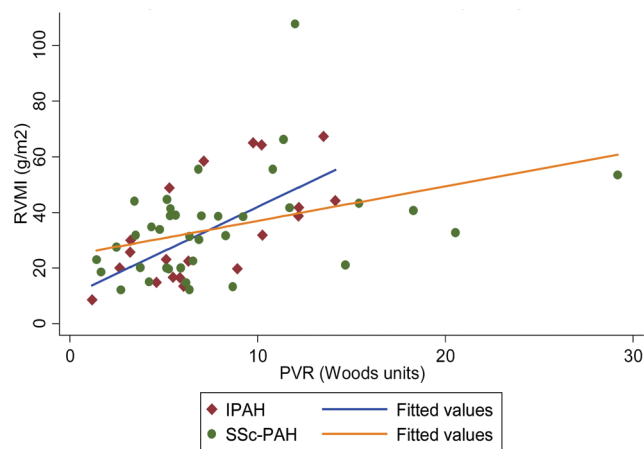


Figure 1. Right ventricular mass index (RVMI) versus pulmonary vascular resistance (PVR) stratified by diagnosis. IPAH: idiopathic pulmonary arterial hypertension; SSc-PAH: scleroderma-associated pulmonary arterial hypertension.

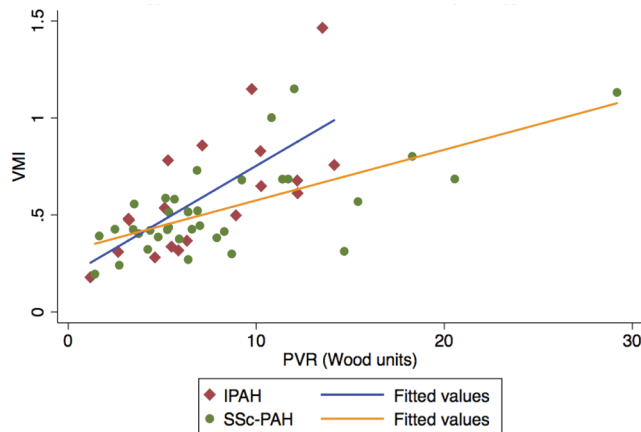


Figure 2. Ventricular mass index (VMI) versus pulmonary vascular resistance (PVR) stratified by diagnosis. IPAH: idiopathic pulmonary arterial hypertension; SSc-PAH: scleroderma-associated pulmonary arterial hypertension.

adaptive hypertrophy and maladaptive hypertrophy. However, our results indicate that measures of RV mass (RVMI and VMI) are linearly associated with multiple measures of RV load. This supports the hypothesis that RV hypertrophy occurs in response to increased load. Moreover, our study supports the notion that disease state modifies the relationship between RV load and RV hypertrophy. We believe this to be valid despite the significant difference in treatment status between groups at time of enrollment in the study. Earlier investigations of PAH-specific therapies have shown reduction in RV mass after several months of therapy.^{32,33} Thus, the IPAH cohort in our study would be more likely to have lower RV mass and, therefore, less likely to demonstrate differences in the relationship between RV hypertrophy and afterload when compared with the SSc-PAH cohort. However, we found clear differences in this relationship between these two groups.

Conclusions

In this cohort of patients with PAH, we found a significant positive relationship between measures of RV morphology on cMRI and invasively measured RV afterload. Furthermore, after adjusting for differences in age, sex, race, BMI, and LV mass, we found that patients with SSc-PAH demonstrate less increase in measures of RV mass with increasing PVR than do patients with IPAH. This suggests a difference in adaptive hypertrophy in patients with SSc-PAH compared with patients with IPAH, which we postulate may contribute to the poor survival associated with SSc-PAH.

Sources of Support: Doris Duke Foundation Scholarship (to BWK), K23 HL092287 and Pulmonary Hypertension Association/National Heart, Lung, and Blood Institute Supplemental Award (to SCM), P50 HL084946 (to PMH), and R01 HL114910 (to PMH and DAK).

Conflict of Interest: SCM has served as a consultant for Actelion and Bayer HealthCare. PMH has served on the advisory boards of Merck, Bayer, and Gilead Sciences.

REFERENCES

1. Simonneau G, Gatzoulis MA, Adatia I, et al. Updated clinical classification of pulmonary hypertension. *J Am Coll Cardiol* 2013;62(25 suppl.): D34–D41.
2. Mukerjee D, St George D, Coleiro B, et al. Prevalence and outcome in systemic sclerosis associated pulmonary arterial hypertension: application of a registry approach. *Ann Rheum Dis* 2003;62(11):1088–1093.
3. Steen VD, Medsger TA. Changes in causes of death in systemic sclerosis, 1972–2002. *Ann Rheum Dis* 2007;66(7):940–944.
4. Hachulla E, Gressin V, Guillemin L, et al. Early detection of pulmonary arterial hypertension in systemic sclerosis: a French nationwide prospective multicenter study. *Arthritis Rheum* 2005;52(12):3792–3800.
5. Tedford RJ, Hassoun PM, Mathai SC, et al. Pulmonary capillary wedge pressure augments right ventricular pulsatile loading. *Circulation* 2012;125(2):289–297.
6. Fisher MR, Mathai SC, Champion HC, et al. Clinical differences between idiopathic and scleroderma-related pulmonary hypertension. *Arthritis Rheum* 2006;54(9):3043–3050.
7. Chung L, Liu J, Parsons L, et al. Characterization of connective tissue disease-associated pulmonary arterial hypertension from REVEAL: identifying systemic sclerosis as a unique phenotype. *Chest* 2010;138(6):1383–1394.
8. Campo A, Mathai SC, Le PJ, et al. Hemodynamic predictors of survival in scleroderma-related pulmonary arterial hypertension. *Am J Respir Crit Care Med* 2010;182:252–260.
9. Forfia PR, Fisher MR, Mathai SC, et al. Tricuspid annular displacement predicts survival in pulmonary hypertension. *Am J Respir Crit Care Med* 2006;174(9):1034–1041.
10. Mathai SC, Sibley CT, Forfia PR, et al. Tricuspid annular plane systolic excursion is a robust outcome measure in systemic sclerosis-associated pulmonary arterial hypertension. *J Rheumatol* 2011;38(11):2410–2418.
11. van de Veerdonk MC, Kind T, Marcus JT, et al. Progressive right ventricular dysfunction in patients with pulmonary arterial hypertension responding to therapy. *J Am Coll Cardiol* 2011;58(24):2511–2519.
12. Tedford RJ, Mudd JO, Girgis RE, et al. Right ventricular dysfunction in systemic sclerosis associated pulmonary arterial hypertension. *Circ Heart Fail* 2013;6(5):953–963.
13. van Wolferen SA, Marcus JT, Boonstra A, et al. Prognostic value of right ventricular mass, volume, and function in idiopathic pulmonary arterial hypertension. *Eur Heart J* 2007;28(10):1250–1257.
14. Swift AJ, Rajaram S, Condliffe R, et al. Diagnostic accuracy of cardiovascular magnetic resonance imaging of right ventricular morphology and function in the assessment of suspected pulmonary hypertension results from the ASPIRE registry. *J Cardiovasc Magn Reson* 2012;14:40.
15. Badano LP, Ghingina C, Easaw J, et al. Right ventricle in pulmonary arterial hypertension: haemodynamics, structural changes, imaging, and proposal of a study protocol aimed to assess remodelling and treatment effects. *Eur J Echocardiogr* 2010;11(1):27–37.
16. Jiang L, Levine RA, Weyman AE. Echocardiographic assessment of right ventricular volume and function. *Echocardiography* 1997;14(2):189–206.
17. Rain S, Handoko ML, Trip P, et al. Right ventricular diastolic impairment in patients with pulmonary arterial hypertension. *Circulation* 2013;128(18):2016–2010.
18. Saba TS, Foster J, Cockburn M, Cowan M, Peacock AJ. Ventricular mass index using magnetic resonance imaging accurately estimates pulmonary artery pressure. *Eur Respir J* 2002;20(6):1519–1524.
19. Chahal H, McClelland RL, Tandri H, et al. Obesity and right ventricular structure and function: the MESA-Right Ventricle Study. *Chest* 2012;141(2):388–395.
20. Kawut SM, Lima JA, Barr RG, et al. Sex and race differences in right ventricular structure and function: the multi-ethnic study of atherosclerosis-right ventricle study. *Circulation* 2011;123(22):2542–2551.
21. Selvin S. *Statistical analysis of epidemiologic data*. 3rd ed. New York: Oxford University Press, 2014.

22. Vonk-Noordegraaf A, Haddad F, Chin KM, et al. Right heart adaptation to pulmonary arterial hypertension: physiology and pathobiology. *J Am Coll Cardiol* 2013;62(25 suppl.):D22–D33.
23. Hopkins WE, Ochoa LL, Richardson GW, Trulock EP. Comparison of the hemodynamics and survival of adults with severe primary pulmonary hypertension or Eisenmenger syndrome. *J Heart Lung Transplant* 1996;15(1 pt. 1):100–105.
24. Hopkins WE. The remarkable right ventricle of patients with Eisenmenger syndrome. *Coron Artery Dis* 2005;16(1):19–25.
25. Cantor WJ, Harrison DA, Moussadji JS, et al. Determinants of survival and length of survival in adults with Eisenmenger syndrome. *Am J Cardiol* 1999;84(6):677–681.
26. van Loon RL, Roofthoof MT, Hillege HL, et al. Pediatric pulmonary hypertension in the Netherlands: epidemiology and characterization during the period 1991 to 2005. *Circulation* 2011;124(16):1755–1764.
27. Rich S, Pogoriler J, Husain AN, Toth PT, Gomberg-Maitland M, Archer SL. Long-term effects of epoprostenol on the pulmonary vasculature in idiopathic pulmonary arterial hypertension. *Chest* 2010;138(5):1234–1239.
28. Johnson RC, Datar SA, Oishi PE, et al. Adaptive right ventricular performance in response to acutely increased afterload in a lamb model of congenital heart disease: evidence for enhanced Anrep effect. *Am J Physiol Heart Circ Physiol* 2014;306(8):H1222–H1230.
29. Mathai SC, Corona-Villalobos CP, Tedford RJ, et al. The relationship between right ventricular contractility and morphology in pulmonary arterial hypertension. *Am J Respir Crit Care Med* 2014;278:A1041.
30. Overbeek MJ, Lankhaar JW, Westerhof N, et al. Right ventricular contractility in systemic sclerosis-associated and idiopathic pulmonary arterial hypertension. *Eur Respir J* 2008;31(6):1160–1166.
31. Opie LH, Commerford PJ, Gersh BJ, Pfeffer MA. Controversies in ventricular remodelling. *Lancet* 2006;367(9507):356–367.
32. Wilkins MR, Paul GA, Strange JW, et al. Sildenafil versus Endothelin Receptor Antagonist for Pulmonary Hypertension (SERAPH) study. *Am J Respir Crit Care Med* 2005;171(11):1292–1297.
33. Chin KM, Kingman M, de Lemos JA, et al. Changes in right ventricular structure and function assessed using cardiac magnetic resonance imaging in bosentan-treated patients with pulmonary arterial hypertension. *Am J Cardiol* 2008;101(11):1669–1672.